

A Density Functional Study of Oxygen Activation by Unsaturated Complexes $[M(\text{bipy})_2]^{2+}$, $M = \text{Cr}$ and Fe

Peter R. Howe and John E. McGrady*

Department of Chemistry, The University of York, Heslington, York YO10 5DD, United Kingdom

Christine J. McKenzie

Department of Chemistry, University of Southern Denmark, Odense Campus, DK-5230 Odense M, Denmark

Received July 23, 2001

Density functional theory is used to probe the reaction of O_2 with the unsaturated transition-metal fragments $[M(\text{bipy})_2]^{2+}$, $M = \text{Cr}, \text{Fe}$. In both cases, calculations indicate that the O_2 molecule is initially trapped as an η^2 -bound superoxide ion, where the unpaired electron in the out-of-plane π^* orbital of O_2 is weakly coupled to those on the trivalent metal ion. In the chromium case, a *cis*-dioxo Cr^{VI} complex is found to be significantly more stable than the superoxo species. The two minima are, however, separated by a large barrier, along with a change in spin state. For the iron analogue, the relative energies of the two minima are reversed, the superoxo complex being the global minimum. The energetics of the O_2 activation processes are consistent with previously reported mass spectrometric experiments, where an adduct, $[M(\text{bipy})_2(\text{O}_2)]^{2+}$, was detected only for chromium.

Introduction

The activation of molecular oxygen has long been a field of active research, primarily due to interest in the metabolism of dioxygen in biological systems. From a simple electronic perspective, the reaction of most organic substrates with O_2 is a spin-forbidden process, rendering them kinetically stable under ambient conditions.¹ An important role for the metalloenzymes that mediate O_2 oxidation chemistry must, therefore, be to overcome the forbidden nature of the reaction by converting the O_2 molecule into a more active oxidizing species.² Over the past decade, the development of density functional theory has made it possible to explore the electronic structure of transition-metal systems, and therefore of metalloenzymes, at a quantitative level.³ Studies of oxygen metabolism have been featured prominently in the early work in this area, and the electronic structure and mechanism of

methane monooxygenase,⁴ cytochrome *c* oxidase,⁵ tyrosinase,⁶ galactose oxidase,⁷ and the oxygen-evolving complex^{2c,8} have all been described in some detail. This work has yielded significant insight into these complex systems, largely through the characterization of stationary points along reaction pathways. However, the large number of atoms required to build a realistic model of such systems precludes an exhaustive survey of potential energy surfaces, particularly when more than one electronic state is involved.

At the opposite end of the spectrum, numerous high-level theoretical studies of O_2 activation by bare metal atoms and cations have also emerged in recent years.⁹ In contrast to the aforementioned metalloenzymes, the simple nature of these gas-phase systems has permitted the characterization

* To whom correspondence should be addressed. E-mail: jem15@york.ac.uk.

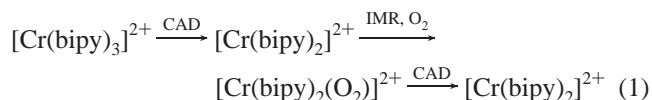
- (1) Filatov, M.; Reckien, W.; Peyerimhoff, S. D.; Shaik, S. J. *Phys. Chem. A* **2000**, *104*, 12014.
- (2) (a) Metz, M.; Solomon, E. I. *J. Am. Chem. Soc.* **2001**, *123*, 4938. (b) Brunold, T. C.; Solomon, E. I. *J. Am. Chem. Soc.* **1999**, *121*, 8288. (c) McGrady, J. E.; Stranger, R. *Inorg. Chem.* **1999**, *38*, 550.
- (3) (a) Siegbahn, P. E. M.; Blomberg, M. R. A. *Chem. Rev.* **2000**, *100*, 421. (b) Holm, R. H.; Kennepohl, P.; Solomon, E. I. *Chem. Rev.* **1996**, *96*, 2239.

- (4) (a) Siegbahn, P. E. M.; Crabtree, R. H. *J. Am. Chem. Soc.* **1997**, *119*, 3103. (b) Basch, H.; Mogi, K.; Musaev, D. G.; Morokuma, K. *J. Am. Chem. Soc.* **1999**, *121*, 7249. (c) Dunitz, B. D.; Beachy, M. D.; Cao, Y.; Whittington, D. A.; Lippard, S. J.; Friesner, R. A. *J. Am. Chem. Soc.* **2000**, *122*, 2828.
- (5) Blomberg, M. R. A.; Siegbahn, P. E. M.; Babcock, G. T.; Wilkström, M. *J. Am. Chem. Soc.* **2000**, *122*, 12848.
- (6) Lind, T.; Siegbahn, P. E. M.; Crabtree, R. H. *J. Phys. Chem. B* **1999**, *103*, 1193.
- (7) Himo, F.; Eriksson, L. A.; Maseras, F.; Siegbahn, P. E. M. *J. Am. Chem. Soc.* **2000**, *122*, 8031.
- (8) (a) Siegbahn, P. E. M.; Crabtree, R. H. *J. Am. Chem. Soc.* **1999**, *121*, 117. (b) Siegbahn, P. E. M. *Inorg. Chem.* **2000**, *39*, 2923.

of complete potential energy surfaces in a number of different electronic states. Perhaps the most important result to emerge from this work is an appreciation of “state-specific reactivity”, where rates and product distributions are determined, at least in part, by the electronic state of the reactants. As an illustrative example, Schröder et al. have shown that the doublet ground state of the CrO_2^+ cation, formed by electron impact on CrO_2Cl_2 , is an active oxidant toward simple hydrocarbons. In contrast, chemical ionization of $\text{Cr}(\text{CO})_6$ in the presence of O_2 yields CrO_2^+ , but in a mixture of several electronic states.^{9a} The authors showed that formation of the doublet ground state of CrO_2^+ from Cr^+ and O_2 in their respective ground states (^5D and $^3\Sigma_g^-$) requires two inter-system crossings, and postulated that the direct activation of O_2 results initially in the formation of an excited quartet state. In marked contrast, the ground state of FeO_2^+ does correlate with ground-state $\text{Fe}^+ + \text{O}_2$, and as a result, a mixture of the two forms an active oxidant.^{9b,c} In a more general sense, the participation of more than one spin state in a reaction has been developed into the concept of “two-state reactivity”, which has received much attention in the recent literature.¹⁰ While the gas-phase chemistry of isolated metal ions is clearly far removed from biological oxygen activation, there seems no reason to suppose that state specificity should not play a role in larger systems. Indeed, Shaik and co-workers have already shown that the concepts developed in the context of gas-phase metal oxo species, $\text{M}=\text{O}^+$, can be extended into the oxidation chemistry of cytochrome P450.¹¹

To make the transition from bare ions into the realm of coordination chemistry, an understanding of the way in which the ligand field influences reactivity by moderating the energies of the different spin states is clearly essential. A recent study of the gas-phase chemistry of coordinatively unsaturated 2,2'-bipyridine (bipy) complexes of a series of divalent metal ions, $[\text{M}(\text{bipy})_2]^{2+}$, $\text{M} = \text{Cr}, \text{Mn}, \text{Fe}, \text{Co}, \text{Ni}, \text{Cu}, \text{Ru}, \text{Os}$,¹² by one of us presents an ideal opportunity to examine this issue. These ions are generated in the gas phase from the solution-derived parent trisbipyridyl complexes by collision-activated dissociation (CAD) using Ar gas. Of the complexes listed above, only those of Cr, Ru, and Os were found to yield detectable concentrations of the oxygen adduct $[\text{M}(\text{bipy})_2(\text{O}_2)]^{2+}$ in subsequent ion–molecule reactions (IMRs) with molecular oxygen. Finally, further CAD of the $[\text{M}(\text{bipy})_2(\text{O}_2)]^{2+}$ ions resulted in the loss of the mass

equivalent of dioxygen in the cases of chromium and ruthenium, but not osmium. The gas-phase reaction sequence for the chromium case is summarized in eq 1. In the context



of the preceding discussion of bare metal cations, the observation of $[\text{Cr}(\text{bipy})_2(\text{O}_2)]^{2+}$, but not its iron analogue, is particularly intriguing, as it provides a direct comparison, at least conceptually, with previous studies on CrO_2^+ and FeO_2^+ ions.⁹

It is important to emphasize that the simple detection of an adduct with empirical formula $[\text{M}(\text{bipy})_2(\text{O}_2)]^{2+}$ provides no structural information, and the connectivity and precise oxidation state of the O_2 unit remain uncertain. Depending on the extent of electron transfer between the metal and ligand, the adduct may adopt any one of the redox isomeric forms $\text{M}^{\text{II}}(\text{O}_2)$, $\text{M}^{\text{III}}(\text{O}_2^-)$, $\text{M}^{\text{IV}}(\text{O}_2^{2-})$, and $\text{M}^{\text{VI}}(\text{O}_2^-)_2$ corresponding to complexes of dioxygen, superoxide, peroxide, and oxide, respectively. The redox noninnocence of the O_2 unit is well documented, and the relative importance of $\text{Fe}^{\text{II}}(\text{O}_2)$, $\text{Fe}^{\text{III}}(\text{O}_2^-)$, and $\text{Fe}^{\text{IV}}(\text{O}_2^{2-})$ forms in hemoglobin, in particular, has been debated at length.¹³ Accurate quantum chemical calculations provide a unique opportunity to probe questions such as redox noninnocence. In addition to yielding structural and spectroscopic parameters for direct comparison with experiment, they provide an intimate picture of the distribution of the electrons. Spin-unrestricted theories are particularly powerful in this context, as they afford a physically correct description of weak coupling between metal and ligand-based electrons as well as conventional covalent bonds. As a result, spin-unrestricted density functional theory has recently been used with some success to explore complexes of redox noninnocent ligands such as the quinone/semiquinone/catecholate triad,¹⁴ as well as dithiolenes¹⁵ and nitrosyl.¹⁶ In this paper, we use spin-unrestricted density functional theory to explore the potential energy surface for O_2 activation on $[\text{Cr}(\text{bipy})_2]^{2+}$. Stationary points are characterized for all possible electronic states, shedding light on the intimate electronic processes involved in the reaction. The corresponding reaction with $[\text{Fe}(\text{bipy})_2]^{2+}$ is also examined, to explore the electronic origins of the different reactivities of the two species. The lack of physical data (structural, spectroscopic) available for the title compounds above makes it difficult to validate the accuracy of the

- (9) (a) Fiedler, A.; Kretzschmar, I.; Schröder, D.; Schwarz, H. *J. Am. Chem. Soc.* **1996**, *118*, 9941. (b) Schröder, D.; Fiedler, A.; Schwarz, J.; Schwarz, H. *Inorg. Chem.* **1994**, *33*, 5094. (c) Schröder, D.; Schwarz, H. *Angew. Chem., Int. Ed. Engl.* **1993**, *32*, 1420. (d) Chertihin, G. V.; Andrews, L.; Bauschlicher, C. W., Jr. *J. Phys. Chem. A* **1997**, *101*, 4026. (e) Elliott, S. D.; Ahlrichs, R. *J. Chem. Phys.* **1998**, *109*, 4267.
- (10) (a) Schröder, D.; Shaik, S.; Schwarz, H. *Acc. Chem. Res.* **2000**, *33*, 139. (b) Shaik, S.; Filatov, M.; Schröder, D. and Schwarz, H. *Chem.—Eur. J.* **1998**, *4*, 193.
- (11) (a) de Visser, S. P.; Ogliaro, F.; Harris, N.; Shaik, S. *J. Am. Chem. Soc.* **2001**, *123*, 3037. (b) Ogliaro, F.; Harris, N.; Cohen, S.; Filatov, M.; de Visser, S. P.; Shaik, S. *J. Am. Chem. Soc.* **2000**, *122*, 8977. (c) Harris, N.; Cohen, S.; Filatov, M.; Ogliaro, F.; Shaik, S. *Angew. Chem., Int. Ed.* **2000**, *39*, 2003.
- (12) Molinda-Svendsen, H.; Bojesen, G.; McKenzie, C. J. *Inorg. Chem.* **1998**, *37*, 1981.

- (13) (a) Momenteau, M.; Reed, C. A. *Chem. Rev.* **1994**, *94*, 659. (b) Bytheway, I.; Hall, M. B. *Chem. Rev.* **1994**, *94*, 639. (c) Summerville, D. A.; Jones, R. D.; Hoffman, B. M.; Basolo, F. *J. Chem. Educ.* **1979**, *56*, 157.
- (14) (a) Adams, D. M.; Noodleman, L.; Hendrickson, D. N. *Inorg. Chem.* **1997**, *36*, 3966. (b) Rodriguez, J. H.; Wheeler, D. E.; McCusker, J. K. *J. Am. Chem. Soc.* **1998**, *120*, 12051. (c) Bachler, V.; Chaudhuri, P.; Wieghardt, K. *Chem.—Eur. J.* **2001**, *7*, 404. (d) Bencini, A.; Daul, C. A.; Dei, A.; Mariotti, F.; Lee, H.; Shultz, D. A.; Sorace, L. *Inorg. Chem.* **2001**, *40*, 1582.
- (15) Fomitchev, D. V.; Lim, B. S.; Holm, R. H. *Inorg. Chem.* **2001**, *40*, 645.
- (16) Rodriguez, J. H.; Xia, Y. M.; Debrunner P. G. *J. Am. Chem. Soc.* **1991**, *113*, 7846.

calculations. We note, however, that density functional theory has been applied, with great success, in a wide range of problems concerned with oxygen activation. For example, the groups of Andrews and Schwarz have shown that, with some exceptions, DFT gives excellent insight into the energetics and vibrational spectroscopy of bare metal adducts of O₂.^{17a-c} In more traditional coordination chemistry, particularly the bioinorganic field, a number of DFT-based studies of oxygen-activating enzymes have emerged in recent years. In these much more complex systems, the agreement with known structural and spectroscopic data is often remarkable.^{17d-g}

Computational Details

All calculations described in this work were performed using the Amsterdam Density Functional (ADF) program developed by Baerends et al.¹⁸ The local density approximation to the exchange potential was used¹⁹ along with the correlation potential of Vosko, Wilk, and Nusair,²⁰ and gradient corrections to exchange (Becke)²¹ and correlation (Perdew).²² A double- ζ Slater-type orbital basis set extended with a single d-type polarization function was used to describe main group elements, while all metals were modeled with a triple- ζ basis. Electrons in orbitals up to and including 1s {O, C, N} and 3p {Cr, Fe} were considered to be part of the core and treated in accordance with the frozen core approximation. Geometries of stationary points were fully optimized using the algorithm of Versluis and Ziegler.²³ No attempt was made to verify that the stationary points were true minima, due to the prohibitive cost of calculating numerical second derivatives. Such calculations were, however, performed for related ligands with the bipyridyl group replaced by the much smaller diimine (C₂N₂H₄) (see the discussion of potential energy surfaces), and no imaginary frequencies were located.

Results and Discussion

[M(bipy)₂]²⁺ Complexes. In the discussion of the binding of O₂, the reference point for all energetic data will be the combined energies of the reactants O₂ + [M(bipy)₂]²⁺ in their respective ground states, optimized structures of which are summarized in Figure 1. For [Cr(bipy)₂]²⁺ (d⁴), the ground state is a quintet, ⁵B₂, with D₂ symmetry. On simple electronic grounds, the d⁴ configuration should favor square planar coordination, but nonbonded interactions between hydrogen atoms on opposite ligands induce a twist of approximately 15° between the two ligand planes. The lowest

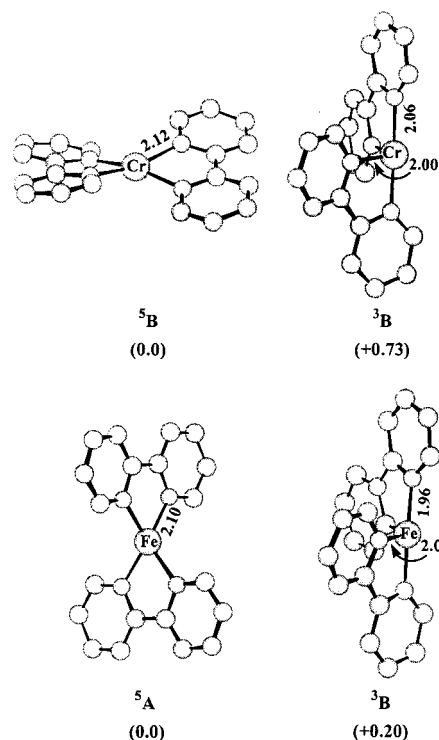


Figure 1. Structures of ground and excited states of [M(bipy)₂]²⁺. Relative energies (eV) are shown in parentheses.

lying excited state, ³B, lies 0.73 eV higher in energy, an indication of the high cost of pairing electrons in the compact 3d orbitals of chromium. The pairing of two electrons forces the complex to adopt a less symmetric, sawhorse-type structure (point group C₂). For the iron complex (d⁶), the ground state is again a quintet, ⁵A, but the occupation of all five d orbitals forces the complex to adopt a more symmetric, pseudotetrahedral structure. Pairing of two electrons to form the first excited state, ³B, again causes a distortion toward a C₂-symmetric structure, but the energetic cost is much lower (0.20 eV) than in the chromium case.

Ion–Molecule Reactions with O₂: [Cr(bipy)₂]²⁺ + O₂.

A preliminary survey of the potential energy surface for [Cr(bipy)₂(O₂)]²⁺ reveals the presence of four distinct minima, ³B, ⁵B, ³A, and ¹A. In all states, the O₂ unit is coordinated in an η² fashion, resulting in C₂ point symmetry. Structural parameters and relative energies for each of the isomers are summarized in Figure 2. The global minimum is the ¹A state (2.56 eV more stable than the separated reactants), where the long O–O separation of 2.57 Å and the short Cr–O bonds (1.60 Å) are characteristic of a Cr^{VI} dioxo species. Attempts to locate a minimum for the corresponding *trans*-dioxo isomer were unsuccessful. The preference for a *cis* arrangement of the two ligands is, however, well established for complexes with a d⁰ configuration, maximizing as it does the donation of π-electron density into the d_π orbitals of the metal.²⁴

The remaining three states, ³B, ⁵B, and ³A, all lie significantly higher in energy, and have much shorter optimized O–O separations. The most stable of the three is ³B, which

- (17) (a) Schröder, D.; Shaik, S.; Schwarz, H. *Struct. Bonding* **2000**, *97*, 91. (b) Wang, X.; Andrews, L. *J. Phys. Chem. A* **2001**, *105*, 5812. (c) Brönstrup, M.; Schröder, D.; Kretzschmar, I.; Schwarz, H.; Harvey, J. N. *J. Am. Chem. Soc.* **2001**, *123*, 142. (d) Brunold, T. C.; Solomon, E. I. *J. Am. Chem. Soc.* **1999**, *121*, 8277. (e) Lam, B. M. T.; Halfen, J. A.; Young, V. G., Jr.; Hagadorn, J. R.; Holland, P. L.; Lledos, A.; Cucurull-Sanchez, L.; Novoa, J. J.; Alvarez, S.; Tolman, W. B. *Inorg. Chem.* **2000**, *39*, 4059. (f) Siegbahn, P. E. M. *J. Am. Chem. Soc.* **1997**, *119*, 3103. (g) Dunietz, B. D.; Beachy, M. D.; Cao, Y.; Whittington, D. A.; Lippard, S. J.; Friesner, R. A. *J. Am. Chem. Soc.* **2000**, *122*, 2828.
- (18) ADF 2.3.0, Theoretical Chemistry, Vrije Universiteit, Amsterdam. (a) Baerends, E. J.; Ellis, D. E.; Ros, P. *Chem. Phys.* **1973**, *2*, 42. (b) te Velde, G.; Baerends, E. J. *J. Comput. Phys.* **1992**, *99*, 84.
- (19) Parr, R. G.; Yang, W. *Density Functional Theory of Atoms and Molecules*; Oxford University Press: New York, 1989.
- (20) Vosko, S. H.; Wilk, L.; Nusair, M. *Can. J. Phys.* **1980**, *58*, 1200.
- (21) Becke, A. D. *Phys. Rev. A* **1988**, *38*, 3098.
- (22) Perdew, J. P. *Phys. Rev. B* **1986**, *33*, 8822.
- (23) Versluis, L.; Ziegler, T. *J. Chem. Phys.* **1988**, *88*, 322.

- (24) (a) Atovmyan, L. O.; Porai-Koshits, M. A. *J. Mol. Struct.* **1969**, *10*, 740. (b) Mingos, D. M. P. *J. Organomet. Chem.* **1979**, *179*, C29.

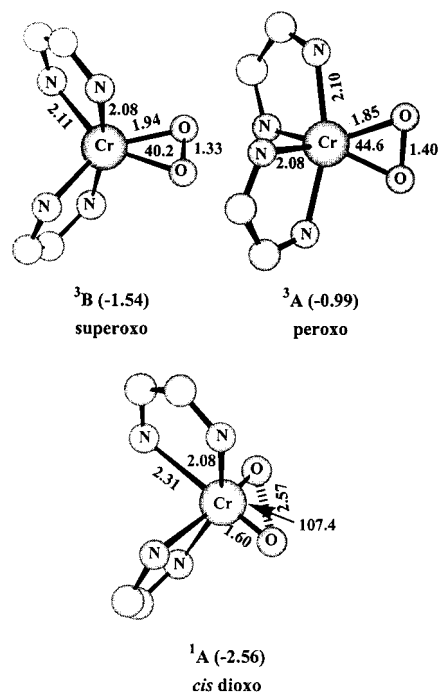


Figure 2. Optimized structures of different states of $[\text{Cr}(\text{bipy})_2(\text{O}_2)]^{2+}$ (the bulk of the bipy ligand has been removed for clarity). Energies (eV), relative to those of the separated reactants, are shown in parentheses.

adopts an approximately trigonal bipyramidal structure with the η^2 -coordinated O_2 unit in the equatorial plane. All attempts to optimize an η^1 -coordinated structure for this state (as well as for ${}^5\text{B}$ and ${}^3\text{A}$) resulted in a return to the η^2 alternative. The optimized O–O separation of 1.33 Å is characteristic of a superoxide, rather than peroxide, ligand, a view that is reinforced by a detailed examination of the electronic structure. The frontier region of the molecular orbital array (Figure 3a) shows three spin- α electrons in the d_π orbitals on the Cr center and a single spin- β electron in an out-of-plane π^* orbital on the O_2 unit, giving rise to net spin densities of +3.07 and -0.51 on Cr and O atoms, respectively. These values are characteristic of an antiferromagnetically coupled $\text{Cr}^{\text{III}}(\text{O}_2^-)$ system, the dominant superexchange pathway being between the d_{xy} orbital on the metal and the out-of-plane π^* orbital of the O_2 unit. The ferromagnetically coupled counterpart of the ${}^3\text{B}$ state, ${}^5\text{B}$, is obtained by flipping the spin of the electron localized on the O_2 unit. This state lies only 0.25 eV above ${}^3\text{B}$, and the two have almost identical structures, consistent with the weak overlap between magnetic orbitals.

It is important to emphasize that the electronic configuration of the ${}^3\text{B}$ state (Figure 3a) does not preclude a $\text{Cr}^{\text{IV}}(\text{O}_2^{2-})$ formulation; the results simply indicate that the alternative $\text{Cr}^{\text{III}}(\text{O}_2^-)$ species is energetically preferred. This conclusion is at first sight somewhat surprising, given the relative paucity of η^2 -bound complexes of superoxide in coordination chemistry.²⁵ Within the confines of C_2 symmetry, it is possible to estimate the magnitude of this

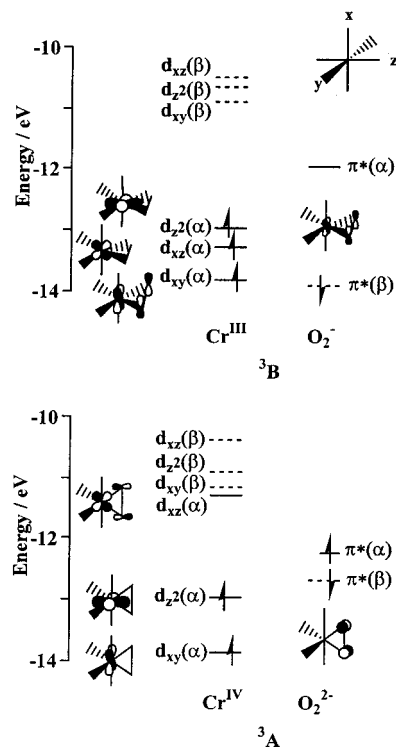


Figure 3. Frontier molecular orbitals of the ${}^3\text{B}$ and ${}^3\text{A}$ states of $[\text{Cr}(\text{bipy})_2(\text{O}_2)]^{2+}$. Spin- α orbitals are shown as full lines, spin- β as broken lines. The spatial distributions of the orbitals (shown schematically) are very similar for the spin- α and spin- β manifolds.

preference (in energetic terms) by forcing the adoption of a peroxo structure. This can be achieved by transferring one electron from the $d_{xz}(\alpha)$ orbital (b symmetry) into $\pi^*(\alpha)$ (a symmetry), the result being an extension of the O–O bond length to 1.40 Å in the ${}^3\text{A}$ state, a value typical of coordinated peroxide. The structural indicator is again confirmed by a detailed examination of the electron distribution (Figure 3b). The frontier region now contains only two occupied spin- α metal-based d orbitals, the third spin- α component of the d_π manifold, $d_{xz}(\alpha)$, being strongly destabilized. On the O_2 unit, both spin- α and - β components of the out-of-plane O_2 π^* orbital are now occupied, leading to net spin densities of +1.84 and +0.12 on Cr and O, respectively. The axial alignment of the peroxide ligand contrasts markedly with the ${}^3\text{B}$ state (superoxide), where an equatorial arrangement was found to be marginally more stable. Moreover, there is a significant rotation barrier in the ${}^3\text{A}$ state (the equatorial rotamer lies 0.41 eV higher in energy), whereas the rotation of the superoxide unit in ${}^3\text{B}$ was almost barrierless (0.02 eV). The absence of a barrier in the latter is a result of the approximate spherical symmetry of the d_π^3 configuration, which permits essentially unhindered rotation of the ligand about the C_2 axis. In the ${}^3\text{A}$ state, in contrast, the vacant spin- α d_{xz} orbital provides a pathway for donation of electrons from the occupied in-plane π^* orbitals of the O_2 unit, but only when it lies in the axial plane.

The separation of 0.55 eV between the two states ${}^3\text{A}$ and ${}^3\text{B}$ indicates that the preference for a superoxo, rather than a peroxo, complex is not a marginal one. (The ${}^3\text{A}$ state represents an upper bound to the energy of the peroxo

(25) (a) Fujisawa, K.; Tanaka, M.; Moro-oka, Y.; Kitajima, N. *J. Am. Chem. Soc.* **1994**, *116*, 12079. (b) Egan, J. W., Jr.; Haggerty, B. S.; Rheingold, A. L.; Sendlinger, S. C.; Theopold, K. H. *J. Am. Chem. Soc.* **1990**, *112*, 2445.

complex; any alternative distribution of the two d electrons within the d_{π} subshell converges to the superoxo ground state.) Moreover, it gives us confidence that the result is not an artifact of the chosen density functional method. While somewhat unexpected on the grounds of the ease of oxidation of chromium, the presence of a $\text{Cr}^{\text{III}}(\text{O}_2^-)$ species is not without precedent, a number of groups having previously postulated their existence.²⁶ Moreover, although the η^2 -mode is relatively uncommon in the coordination chemistry of the superoxide ion, computational studies indicate that such complexes are relatively common in gas-phase chemistry of bare metal atoms and ions.⁹ In this context, the highly unsaturated $[\text{M}(\text{bipy})_2]^{2+}$ fragments have closer links to gas-phase, rather than solution- and solid-state, coordination chemistry.

Having fully characterized the minima of the various electronic states, we can now survey 1-dimensional potential energy curves (Figure 4), and hence consider the likely nature of the adduct observed in the mass spectrometric experiment. The reaction coordinate is defined as the O–O distance, and all other parameters are treated as variables. This procedure necessarily involves a large number of calculations, and would be prohibitively expensive for the complete molecule $[\text{M}(\text{bipy})_2(\text{O}_2)]^{2+}$. The potential energy curves were consequently generated using the diimine $\text{C}_2\text{N}_2\text{H}_4$ rather than the full bipyridyl ligand. This simplification has obvious drawbacks, most notably the localization of double bond character in the $\text{C}=\text{N}$ bond. However, the structures of the CrO_2 units in each of the four minima ^1A , ^3B , ^5B , and ^3A are very similar to those in Figure 2, where the full bipyridyl ligand was used. Moreover, the energetic ordering is unchanged ($^1\text{A} < ^3\text{B} < ^5\text{B} < ^3\text{A}$), suggesting that no major artifacts are introduced by the use of the diimine. The use of the simplified ligand also makes possible the calculation of vibrational frequencies, a procedure that was clearly intractable for the full $[\text{M}(\text{bipy})_2(\text{O}_2)]^{2+}$ species (63 atoms). The absence of imaginary frequencies confirms all four optimized structures, ^1A , ^3B , ^5B , and ^3A , as true minima. The striking similarity (both structural and energetic) between the complexes with the full bipyridyl ligand and those with the simplified diimine provides indirect evidence that the former are also true minima.

The separated reactants $[\text{Cr}(\text{bipy})_2]^{2+}$ and O_2 in their respective ground states (^5A and $^3\Sigma_g^-$) correlate with the triplet and quintet states of $[\text{Cr}(\text{bipy})_2(\text{O}_2)]^{2+}$. In contrast, the singlet dioxo species correlates with an excited triplet state of $[\text{Cr}(\text{bipy})_2]^{2+}$, suggesting that the trapping of dioxygen should occur, at least initially, along the triplet spin surface, yielding the metastable Cr^{III} superoxo complex ^3B . From this metastable state, cleavage of the O–O bond to form the thermodynamic product ^1A involves a significant barrier, as well as a change in spin state. The kinetic influence of the intersystem crossing is not clear, but even if the

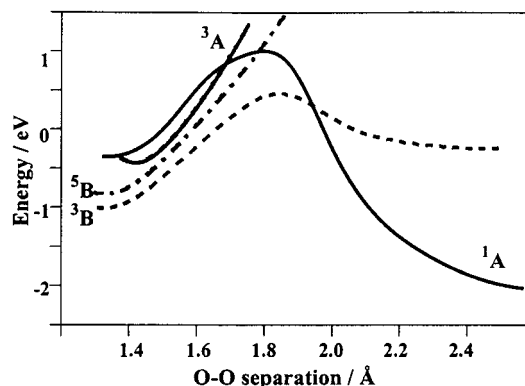


Figure 4. Potential energy curves for the various states of $[\text{Cr}(\text{C}_2\text{N}_2\text{H}_4)_2(\text{O}_2)]^{2+}$. The zero point is taken to be the sum of the energies of the two reactants in their respective ground states.

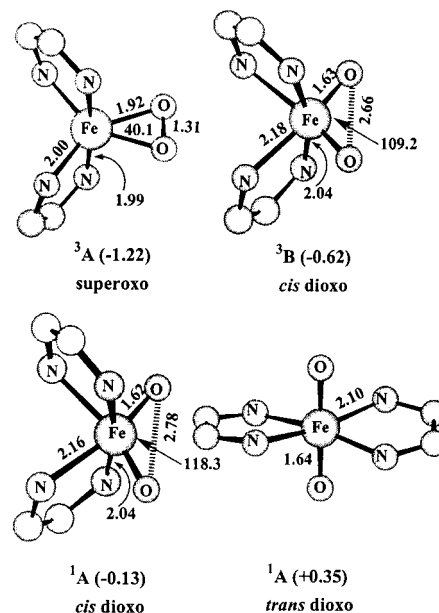


Figure 5. Optimized structures of different states of $[\text{Fe}(\text{bipy})_2(\text{O}_2)]^{2+}$ (the bulk of the bipy ligand has been removed for clarity). Energies (eV), relative to those of the separated reactants, are shown in parentheses.

transition between spin surfaces is very rapid, the ~ 1 eV required to reach the minimum energy crossing point (the one-dimensional potential energy surface provides a lower bound to the minimum energy crossing point) may be sufficient, at least at ambient temperatures, to retard cleavage of the O–O bond. The potential energy curve therefore appears to offer two plausible structures for the observed adduct $[\text{Cr}(\text{bipy})_2(\text{O}_2)]^{2+}$, a metastable Cr^{III} superoxo complex and the thermodynamic product, a *cis*-dioxo Cr^{VI} species. We will consider these two possibilities in detail following a review of the analogous Fe system, where, significantly, no adduct was observed.

$[\text{Fe}(\text{bipy})_2]^{2+} + \text{O}_2$. Optimized structural parameters and relative energies of the various minima located on the potential energy surface of $[\text{Fe}(\text{bipy})_2(\text{O}_2)]^{2+}$ are summarized in Figure 5. The structural features are, in general, very similar to those found for the chromium analogue, but significant differences emerge when their relative energies are considered. At short O–O separations, the most stable species is a triplet (^3A) state with an O–O separation of 1.32 Å, very

(26) (a) Dickman, M. H.; Pope, M. T. *Chem. Rev.* **1994**, *94*, 569. (b) Ozawa, T.; Hanaki, A. *Inorg. Chim. Acta* **1988**, *147*, 103. (c) Kellerman, R.; Hutta, P. J.; Klier, K. *J. Am. Chem. Soc.* **1974**, *96*, 5946. (d) Cheung, S. K.; Grimes, C. J.; Wong, J.; Reed, C. A. *J. Am. Chem. Soc.* **1976**, *98*, 5028. (e) Bakac, A.; Scott, S. L.; Espenson, J. H.; Rodgers, K. R. *J. Am. Chem. Soc.* **1995**, *117*, 6483.

similar to that in the ^3B and ^5B states of $[\text{Cr}(\text{bipy})_2(\text{O}_2)]^{2+}$. The net spin densities of +1.21 and +0.40 on Fe and O, respectively, are consistent with its formulation as a ferromagnetically coupled superoxo complex of low-spin Fe^{III} . The antiferromagnetically coupled analogue ^1A (net spin densities of +0.96 and -0.49) lies 0.06 eV higher in energy, and again has an almost identical structure. The switch from antiferromagnetic (chromium) to ferromagnetic (iron) coupling in the ground state of the superoxo complex is caused by the two additional electrons in iron, which occupy the $d_{xy}(\beta)$ and $d_{xz}(\beta)$ orbitals shown in Figure 3. The occupation of the spin- β component of d_{xy} effectively cuts off the main superexchange pathway between the metal and the out-of-plane π^* orbital of the superoxide ion. The only remaining vacant spin orbital in the metal manifold, $d_z^2(\beta)$, is almost orthogonal to the out-of-plane π^* orbital, giving rise to the ferromagnetic coupling.

At larger O–O separations (2.67 Å), the most stable structure again corresponds to a *cis*-dioxo isomer, in this case a triplet, ^3B , consistent with the d^2 configuration of Fe^{VI} . Minima were also located for a *trans*-dioxo isomer, $^1\text{A}(\text{trans-dioxo})$ (optimized in D_2 point symmetry), and a singlet *cis*-dioxo species, $^1\text{A}(\text{cis-dioxo})$, but both were found to be considerably less stable than ^3B (by 0.97 and 0.49 eV, respectively). This observation is slightly surprising, as a *trans* orientation prevails in the majority of dioxo complexes with a d^2 configuration.²⁷ Moreover, in the few cases where a *cis* arrangement of the oxo ligands is preferred, the complexes are diamagnetic rather than paramagnetic.²⁸ The stabilities of both the *trans*-dioxo and diamagnetic *cis*-dioxo complexes have been rationalized in terms of orbital overlap, π -donation from the oxo ligands dominating in the former, and π back-donation to other ligands in the latter.²⁹ Such arguments have, however, been developed in the context of second- and third-row transition metals, where the metal-based orbitals are relatively diffuse. In contrast, the very contracted 3d orbitals of Fe^{VI} afford relatively weak overlap with both oxo and bipyridyl ligands, and also result in very strong repulsions between the two remaining d electrons. Thus, the more efficient π bonding in the singlet states (*cis* or *trans*) is not sufficient to offset the unfavorable effect of pairing the two electrons in a single orbital, and a triplet ground state is preferred. In contrast, preliminary calculations on the osmium analogue indicate that the π orbital overlap with the oxo ligands dominates, rendering the *trans*-dioxo isomer more stable, in accord with experimental results.^{26a} Whatever the nature of the $\text{Fe}^{\text{VI}}(\text{O}^{2-})_2$ species, the most significant point is that, in marked contrast to its chromium analogue, it is considerably *less* stable than the alternative

$\text{Fe}^{\text{III}}(\text{O}_2^-)$, ^3A . The superoxo complex is also almost 0.3 eV less stable, relative to the separated reactants, than its chromium analogue (^3B).

Discussion and Summary

In this paper, we have surveyed the potential energy surfaces for O_2 activation on a pair of closely related unsaturated transition-metal fragments, $[\text{Cr}(\text{bipy})_2]^{2+}$ and $[\text{Fe}(\text{bipy})_2]^{2+}$. The qualitative features of the surfaces are very similar: the O_2 molecule is initially trapped as an η^2 -bound superoxide radical, with weak magnetic coupling between the unpaired electrons on the metal and ligand (antiferromagnetic and ferromagnetic in chromium and iron, respectively). In both systems, an additional minimum, corresponding to a *cis*-dioxo species, was located. For the chromium complex, the dioxo species is more stable than its superoxo counterpart, while the reverse is true for iron.

In the original report of the CAD experiment,¹² we interpreted the dissociation of O_2 from the Cr species as evidence that the O–O bond was not completely cleaved in the adduct. We are now in a position to critically evaluate this proposal in light of the calculated energetics of the system. As noted previously, there are two minima on the surface, the initially formed, metastable, Cr^{III} superoxide (^3B) and the global minimum, the *cis*-dioxo Cr^{VI} (^1A), either of which might be the dominant species in the gas phase. Without a detailed analysis of the energy dependence of the cross-section for CAD, we cannot make an accurate assessment of the binding energy for the O_2 molecule. Nevertheless, it is clear that while the overall binding energy of the O_2 unit in the *cis*-dioxo species is relatively large (2.56 eV), it is not sufficient to preclude the possibility that dissociation of O_2 might occur under the prevailing reaction conditions. Thus, we are forced to conclude that the CAD experiments do not allow us to distinguish between the ^3B and ^1A states of $[\text{Cr}(\text{bipy})_2(\text{O}_2)]^{2+}$, and hence to make a definitive statement as to whether the O–O bond is cleaved in the adduct. The comparison between the chromium system and its iron analogue, where no adduct is observed, is illuminating in this context. If the dominant gas-phase species were the metastable Cr^{III} superoxo species (^3B), then it would be difficult to rationalize the failure to observe a signal for the analogous iron species (^1A), which is only 0.32 eV less stable, relative to the reactants. The *cis*-dioxo Cr^{VI} species, in contrast, is over 1 eV more stable than any high- or low-valent adduct of the iron system. The fact that the potential energy surfaces of the chromium and iron systems differ significantly only at higher oxidation states, combined with the failure to detect an adduct of the iron complex, leads us to favor the conclusion that the dominant species in the gas phase is the *cis*-dioxo Cr^{VI} complex.

Acknowledgment. The Engineering and Physical Sciences Research Council (U.K.) are gratefully acknowledged for financial support.

IC010782C

(27) Holm, R. H. *Chem. Rev.* **1987**, *87*, 1401.

(28) (a) Dobson, J. C.; Takeuchi, K. J.; Pipes, D. W.; Geselowitz, D. A.; Meyer T. J. *Inorg. Chem.* **1986**, *25*, 2375. (b) Cheng, W.-C.; Yu, W.-Y.; Cheung, K.-K.; Che, C.-M. *J. Chem. Soc., Chem. Commun.* **1994**, 1063.

(29) (a) Demachy, I.; Jean, Y. *Inorg. Chem.* **1997**, *36*, 5956. (b) Demachy, I.; Jean, Y. *Inorg. Chem.* **1996**, *35*, 5027.